sciendo

Mechanics and Mechanical Engineering 2019; 23:23–27

Research Article

N. Manopradha*, S. Rama, S. Gowri, K. Kirubavathi, and K. Selvaraju

# Theoretical Investigation on Growth Kinetics and Thermodynamic Properties of Pyridine-2-Carboxylic Acid Crystals

https://doi.org/10.2478/mme-2019-0004
Received Apr 21, 2018; revised Oct 1, 2018; accepted Nov 20, 2018

**Abstract:** This work illustrates the significance of kinetic parameters of nucleation and thermal decomposition for Pyridine-2-carboxylic acid crystals. In the interest of maximizing the growth condition for the production of single crystals, nucleation parameters such as interfacial energy ($\sigma$), volume free energy ($\Delta G_V$), critical energy barrier for nucleation ($\Delta G^\star$), radius of the critical nucleus ($r^\star$) and nucleation rate (J) were determined from the classical nucleation theory of solubility-enthalpy relation. The optimized geometry of the compound was computed from the DFT-B3LYP gradient calculations employing 6-31G(d,p) basis set and its vibrational frequencies were evaluated. Based on the vibrational analysis, the thermodynamic parameters were obtained and the correlative equations between these thermodynamic properties and variation in temperatures were also reported.

**Keywords:** Nucleation kinetics, growth from solution, DFT

## 1 Introduction

Pyridine-2-carboxylic acid (2PA) are used as building blocks in crystal engineering and many coordination polymers. These are beneficial compounds for human organism and are also involved in several essential biochemical processes. 2PA has been used as a valuable chelating agent. [1] It is not only a potential proton acceptor but also a proton donor depending on the deprotonated groups. [2] The growth aspects of pyridine-2-carboxylic crystals have been studied in the past, but there are no reports on the nucleation kinetics and DFT study of this organic material. In the present work, the nucleation parameters such as interfacial energy ($\sigma$), volume free energy ($\Delta G_V$), critical energy barrier for nucleation ($\Delta G^\star$), radius of the critical nucleus ($r^\star$) and nucleation rate (J) were evaluated. [3] The thermodynamic parameters from the vibration analysis were compared to the enthalpy obtained from solubility to predict the stability of the crystal.

DFT methods were performed to acquire the vibration information on the optimized geometry, relationships between molecular structure, hydrogen bonding and hyperpolarizability, and thus, non-linear response of the title compound was obtained. This can be used to support the effort towards the discovery of new efficient materials for technological applications by the design strategy for engineering of crystals with predesigned architecture, especially, in the field of nonlinear optics. [4]

## 2 Nucleation Kinetics

Nucleation study is useful to interpret proper supersaturation to provide controlled nucleation rate to obtain good quality single crystals. [5] The concept of nucleation kinetics was introduced by Gibbs. Nucleation is the initial process that occurs in the formation of a crystal from a solution, in which a small number of ions become arranged in a pattern, forming a site on which additional particles are deposited as the crystal grows. To generate a new nucleus from the parent phase, the nucleation process must overcome the potential barrier; this is done using the process of super saturation, which results in the formation of seed nuclei. The process of nucleation is controlled by nucleation rate parameter, which plays a key role in new phase formation.

At the solution– crystal interface, the interfacial energy is formed, which is a crucial parameter in the theo-

---

***Corresponding Author: N. Manopradha:** Department of Physics, Cauvery College for Women, Tiruchirappalli - 620 018, India; Email: mano.pradha@gmail.com

**S. Rama:** Department of Physics, Agni College of Technology, Chennai - 600 130, India

**S. Gowri:** Department of Physics, Cauvery College for Women, Tiruchirappalli - 620 018, India

**K. Kirubavathi, K. Selvaraju:** PG & Research Department of Physics, Govt. Arts College, Ariyalur - 621 713, India

ries of nucleation and crystal growth. However, certain difficulties were encountered in the nucleation experiments such as the requirement of a solution free from foreign particles, volume of the solution and so on. Theoretical attempts have been made by several researchers to estimate the interfacial energy using solubility data.

Interfacial energy of the solid and liquid interface is an important phenomenon in the nucleation process. Based on the solution kinetics theory, Bennema and Sohnel [6] have derived an expression that explains the linear dependence of interfacial energy ($\sigma$) on solubility:

$$\sigma = (kT/d^2)[0.173 - 0.248 \ln \chi_m] \tag{1}$$

where, $\sigma$ - interfacial energy (J/m$^2$); k - Boltzmann constant (J K$^{-1}$); T - Temperature in (K); d - mean molar ionic diameter in crystal = $\{(6/\pi)v\}^{1/3}$; $\chi_m$ - mole fraction of solute in solution.

The relation between solubility and enthalpy of a real solution is given as: [7]

$$\ln \chi_m = (-\Delta H_s/RT) + (\Delta S_E/R) \tag{2}$$

$\Delta H_s$ - Enthalpy of fusion (J mol$^{-1}$)
R - Gas constant (J K$^{-1}$mol)
$\Delta S_E$ - Excess entropy of mixing.

From the reported nucleation kinetics equations, nucleation parameters such as interfacial energy ($\sigma$), volume free energy ($\Delta G_v$), critical energy barrier for nucleation ($\Delta G^*$), radius of the critical nucleus ($r^*$) and nucleation rate ($J$) of 2PA crystal was calculated for various temperatures with constant variation in the super saturation ratio and vice versa.

# 3 Experimental

## 3.1 Materials and methods

The chemical used in this experiment was an analytical reagent as received from the commercial sources without further purification. Pyridine-2-carboxylic acid was purchased from Alfa Aesar. The solubility studies of 2PA were carried out in a constant temperature bath with temperature accuracy ± 0.01°C. The solute was added to double distilled water until the saturation condition was reached. The equilibrium concentration of the solute was analyzed gravimetrically. The experiment was repeated at different temperatures.

## 3.2 Computational Methods

GAUSSIAN 09 quantum chemical software [8] was used for all the calculations. The molecular structure of pyridine-2-carboxylic acid was optimized by Berny's optimization algorithm using redundant internal co-ordinates at the DFT level, using the closed-shell Becke–Lee–Yang–Parr hybrid exchange-correlation three-parameter functional (B3LYP) in combination with 6-31G(d,p) basis set to derive the complete geometry optimizations and normal mode analysis on isolated entities. [9–11] The frontier molecular orbitals (HOMO and LUMO) are generated at DFT/B3LYP/6-31G(d,p) level to explain the electronic and optical properties. The important quantum chemical molecular properties, that is, the global reactivity descriptors have been calculated using the highest occupied molecular orbital (HOMO) and lowest unoccupied molecular orbital (LUMO). [12–17]

The first hyperpolarizability ($\beta$) and the static polarizability ($\alpha$) of 2PA have been predicted using the DFT/B3LYP/6-31G(d,p) method. Using the third rank tensor, the 27 components of 3D matrix can be reduced to 10 components due to the Kleinmann symmetry. [18, 19] The output from Gaussian 09 provides ten components of this matrix as $\beta_{xxx}$, $\beta_{yxx}$, $\beta_{xyy}$, $\beta_{yyy}$, $\beta_{zxx}$, $\beta_{xyz}$, $\beta_{zyy}$, $\beta_{xzz}$, $\beta_{yzz}$, $\beta_{zzz}$, respectively. The following equation renders the results of components of first hyperpolarizability:

$$\beta = (\beta_x^2 + \beta_y^2 + \beta_z^2)^{1/2} \tag{3}$$

where,
$\beta_x = \beta_{xxx} + \beta_{xyy} + \beta_{xzz}$; $\beta_y = \beta_{yyy} + \beta_{yxx} + \beta_{yzz}$; $\beta_z = \beta_{zzz} + \beta_{zxx} + \beta_{zyy}$

The equations for calculating the magnitude of static polarizability is defined as follows:

$$\alpha_o = (\alpha_{xx} + \alpha_{yy} + \alpha_{zz})/3 \tag{4}$$

# 4 Results and Discussion

## 4.1 Metastable zone width (MZW)

The knowledge of MZW will help us in the selection of an optimum rate of supersaturation generation to avoid the exercise for secondary nucleation. The difference between the equilibrium temperature and nucleation temperature in the nucleation curve is called the metastable zone width. The nucleation temperature for each saturation temperature can be calculated using the data represented in Figure 1.

**Table 1:** Nucleation Table from Picolinic Acid for Super Saturation Ratio-1.1

| T (K) | $\Delta G_V$ (J/m$^3$) | $\sigma$ (J/m$^2$) | ΔG* (J) | $r^*$ (m) | $i^*$ | J (nuclei/m$^3$/sec) |
|---|---|---|---|---|---|---|
| 304 | −2.543050e+006 | 0.006923 | 8.592447e−019 | 5.444707e−009 | 4.297886e+003 | 8.300411e+012 |
| 308 | −2.576511e+006 | 0.003852 | 1.442422e−019 | 2.990478e−009 | 7.121199e+002 | 2.503985e+012 |
| 316 | −2.643433e+006 | 0.002345 | 3.090731e−020 | 1.774264e−009 | 1.487256e+002 | 8.814279e+011 |
| 321 | −2.685260e+006 | 0.001556 | 8.754144e−021 | 1.159123e−009 | 4.146868e+001 | 3.761922e+011 |

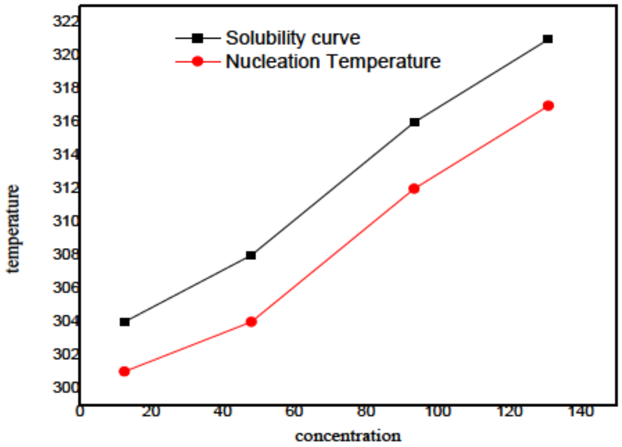

**Figure 1:** Solubility curve for 2PC

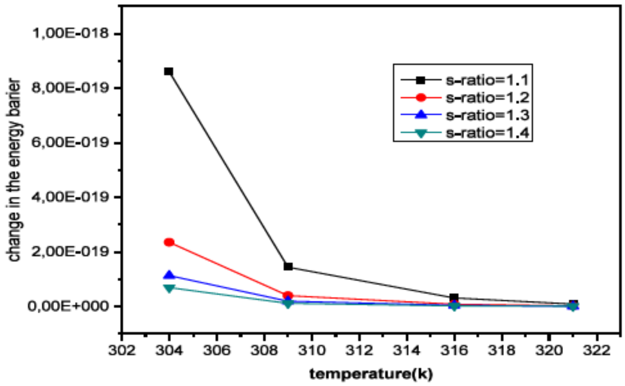

**Figure 2:** Variation of Gibbs free energy with supersaturation and temperature for 2PA

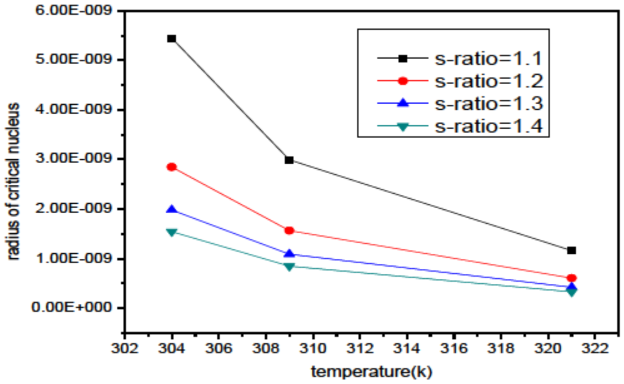

**Figure 3:** Variation of radius of critical nucleus with temperature and supersaturation ratio of 2PA

In this work, the theoretically calculated values of metastable zone width for the crystallization temperatures of crystals using the slow evaporation method have been reported for the first time. From the results, it is observed that the zone width is narrow at lower temperatures and broader at higher temperatures. Table 1 enlists the estimated nucleation parameters of 2PA with different temperatures. The change in free energy per unit volume ($\Delta G_V$) decreases with an increase in the supersaturation, which drives the crystallization process. Figure 2 shows the variation of energy barrier ($\Delta G^*$) with respect to temperature. Figure 3 shows the change in critical radius ($r^*$) as a function of temperature as well as the supersaturation. Decrease in interfacial energy ($\sigma$) (as shown in Table 1) with higher values of temperature leads to a decrease in the radius of the critical nuclei and causes the decreases in the free energy of the system. From the classical nucleation theory diagram, this implies that volume free energy decreases and surface free energy increases, which starts the growth of the crystal.

## 4.2 Equilibrium Concentration of Pyridine-2-carboxylic acid crystals

The solubility data of Pyridine-2-carboxylic acid crystal is fitted to a second order polynomial equation form for all the equilibrium temperatures. [20]

$$C_{sat} = -0.0312746T^2 + 26.2771T - 5083.14 \quad (5)$$

Correlative equation (5) is used to obtain the saturation concentration of any temperature for Pyridine-2-carboxylic acid crystals. Table 2 shows that there is a de-

**Table 2:** Thermodynamics values

| T (K) | S (J/mol.K) | Cp (J/mol.K) | ddH (kJ/mol) | Gibbs free energy (j) |
|---|---|---|---|---|
| 304 | 355.16 | 120.69 | 21.64 | −107947 |
| 308 | 357.33 | 122.12 | 22.12 | −110035.52 |
| 316 | 360.5 | 124.96 | 23.11 | −113894.89 |
| 321 | 362.48 | 126.73 | 23.74 | −116332.34 |

cline in the Gibbs free energy with an increase in the temperature. This enhances the growth of the crystal.

### 4.3 Frontier molecular orbital analysis

The energy gap of HOMO-LUMO explains the eventual charge transfer interactions within the conformers. The HOMO and LUMO energies of 2PA, as calculated by DFT/B3LYP/6-31G(d,p) method, are as follows:
HOMO energy, $E_{HOMO}$ = −7.092eV
LUMO energy, $E_{LUMO}$ = −1.630eV
HOMO-LUMO energy gap, [22] $\Delta E_{GAP} = E_{LUMO} - E_{HOMO}$ = 5.46118eV

The gap between HOMO and LUMO has been used to prove the bioactivity from intramolecular charge transfer. The plots of HOMO and LUMO are shown in Figure 4. The computed high value of HOMO-LUMO energy gap (5.46118 eV) in 2PA confirms the chemical stability of the molecule. [21–25] The global reactivity descriptors, such as ionization potential (I), electron affinity (A), electrophilicity index ($\omega$), chemical hardness ($\eta$), softness (S) and chemical potential ($\mu$), have been calculated using the energy of HOMO and LUMO. The values are listed in Table 3.

**Table 3:** Calculated quantum chemical molecular orbital properties for 2PA using the DFT/B3LYP/6-31G(d,p) method

| Parameters | B3LYP/6-31G(d,p) |
|---|---|
| ionization potential (I) | 7.092eV |
| electron affinity (A) | 1.630eV |
| chemical hardness ($\eta$) | 2.730eV |
| chemical potential ($\mu$) | −4.361eV |
| electrophilicity index ($\omega$) | 3.483eV |
| softness (S) | 0.366 $eV^{-1}$ |

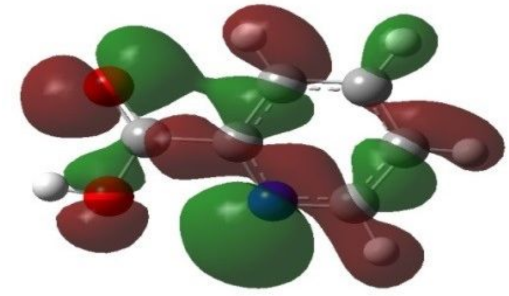

**(a)** Homo

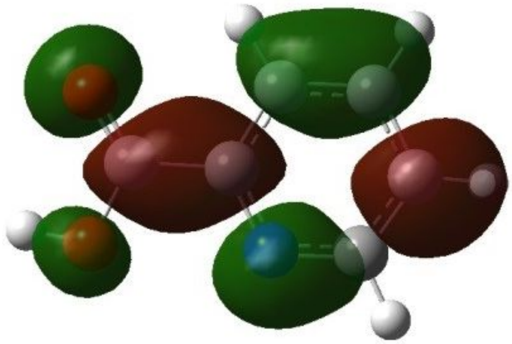

**(b)** Lumo

**Figure 4:** HOMO and LUMO plot of 2PA

### 4.4 NLO studies – First order hyperpolarizability

The values of $\alpha_o$ and $\beta$ components of the Gaussian 09w output are reported in atomic units (a.u.); and the calculated values should be converted into electrostatic units (esu). The polarizability and the first hyperpolarizability of 2PA are 1.0405 x $10^{-23}$ esu and 4.1027 x $10^{-31}$ esu, respectively. The first hyperpolarizability of the title compound is 1.1 times greater than those of urea ($\beta$ of urea is 0.3728 x $10^{-30}$ esu obtained by HF/6-311G(d,p) method).

## 5 Conclusion

The study evaluates the nucleation parameters of the title compound. The interfacial energy and the energy barrier for nucleation decreases with an increase in temperature. The values of kinetic parameters obtained by the application of different equations are in good agreement with each other. This confirms that the evaluated nucleation parameters are feasible for the growth of 2PA crystals. The first-order hyperpolarizability, polarizability and quantum chemical molecular orbital properties of 2PA are computed at the DFT level and the results are discussed.

# References

[1] S. Gowri, T. Uma Devi, D. Sajan, C. Surendra Dilip, A. Chandramohan, N. Lawrence, Crystal growth, spectral, optical and thermal properties of semiorganic nonlinear optical material: Picolinic acid hydrochloride Spectrochimica Acta, Part A: Molecular and Bi molecular Spectroscopy, 110, 28–35, 2013.

[2] Di Li and Guo-Qing Zhong, Synthesis, Crystal Structure, and Thermal Decomposition of the Cobalt(II) Complex with 2-Picolinic Acid, Hindawi Publishing Corporation, The Scientific World Journal, 7 pages, 2014.

[3] S. Rama, C.Surendra Dilip, Rajesh Narayana Perumal, Evaluation of kinetic parameters for water soluble crystals by thermo gravimetric analysis, Journal of Crystal Growth, 409, 32–38, 2015.

[4] V. Sasikala, D. Sajan, N. Vijayan, K. Chaitanya, M. S. Babu Raj, B.H. Selin Joy, Electronic structure, vibrational spectral and intervening orbital interaction studies of NLO material: Guanidium 4-nitrobenzoate, Spectrochimica Acta, Part A: Molecular and Biomolecular Spectroscopy, 123, 127–141, 2014.

[5] K. Selvaraju, K. Kirubavathi, N. Vijayan, S. Kumararaman, Investigations on the nucleation kinetics of bis glycine sodium nitrate, Journal of Crystal Growth, 310, 2859–2862, 2008.

[6] P. Bennema, O. Sohnel, Interfacial surface tension for crystallization and precipitation from aqueous solutions, Journal of Crystal Growth, 102, 547–556, 1990.

[7] U. Rychlewska, Chiral recognition in salts of trans-1,2-diaminocyclohexane and optically active tartaric acids: crystal structure of 1:2 salt of (S,S)-diaminocyclohexane with (R,R)-tartaric acid, Journal of Molecular Structure, 474, 235–243, 1999.

[8] A.D. Becke, Density-functional thermochemistry. I. The effect of the exchange-only gradient correction, Journal of Chemical Physics, 98 (7), 5648–5652, 1993.

[9] C. Lee, W. Yang, R. G. Parr, Development of the Colle-Salvetti correlation-energy formula into a functional of the electron density, Physics Review B, 37, 785–789, 1988.

[10] P. Perdew, Y. Wang, Accurate and simple analytic representation of the electron-gas correlation energy, Physics Review B, 45, 13244–13249, 1992.

[11] R.G. Parr, W. Yang, Density Functional Theory for Atoms and Molecules, Oxford University Press, New York, 1989.

[12] T.A. Koopmans, Über die Zuordnung von Wellenfunktionen und Eigenwerten zu den Einzelnen Elektronen Eines Atoms, Physica, 1, 104–113, 1933.

[13] Jane S. Murray, Fakhr Abu-Awwad and Peter Politzer, Prediction of Aqueous Solvation Free Energies from Properties of Solute Molecular Surface Electrostatic Potentials, Journal of Physical Chemistry A, 103 (12), 1853–1856, 1999.

[14] R.S. Mulliken, A new electroaffinity scale; together with data on valence states and on valence ionization potentials and electron affinities, Journal of Chemical Physics, 2, 782–793, 1934.

[15] R.G. Pearson, Absolute electronegativity and hardness: applications to organic chemistry Journal of Organic Chemistry 54, 1423–1430, 1989.

[16] V. Balachandran, A. Nataraj, T. Karthick, Comparative vibrational spectroscopic studies, HOMO-LUMO, NBO analyses and thermodynamic functions of p-cresol and 2-methyl-p-cresol based on DFT calculations Spectrochimica Acta, Part A: Molecular and Bi molecular Spectroscopy , 104, 114–129, 2013.

[17] D.A. Kleinman, Nonlinear Dielectric Polarization in Optical Media, Physical Review, 126, 1977–1979, 1962.

[18] H. Tanak, Y. Koysal, S_. Is_ık, H. Yaman, V. Ahsen, Experimental and Computational Approaches to the Molecular Structure of 3-(2-Mercaptopyridine)phthalonitrile, Bull. Korean Chem. Soc., 32 (2), 673–680, 2011.

[19] S. Rama, C. Surendra Dilip, Rajesh Narayana Perumala, A software program to investigate the nucleation kinetics of solution grown crystals using MATLAB platform, Computer Physics Communications 185, 661–669, 2014.

[20] N. Tagmatarchis, E. Aslanis, K. Prassides, H. Shinohara, Mono-, Di- and Trierbium Endohedral Metallofullerenes: Production, Separation, Isolation, and Spectroscopic Study, Chemistry of Materials, 13, 2374–2379, 2001.

[21] Z. Zhou, R.G. Parr, Activation hardness: new index for describing the orientation of electrophilic aromatic substitution, Journal of the American Chemical Society, 112, 5720–5724, 1990.

[22] J. Gilman, Chemical and physical “hardness”, Materials Research Innovations, 1, 71–76, 1997.

[23] J. Aihara, Reduced HOMO-LUMO Gap as an Index of Kinetic Stability for Polycyclic Aromatic Hydrocarbons, Journal of Physical Chemistry A, 103, 7487–7495, 1999.

[24] J. Aihara, Why are some polycyclic aromatic hydrocarbons extremely reactive?, Physical Chemistry Chemical Physics, 1, 3193–3197, 1999.

[25] J. Aihara, Weighted HOMO-LUMO energy separation as an index of kinetic stability for fullerenes, Theoretical Chemistry Accounts, 102, 134-138, 1999.